

Energetics of idealized hurricane-like vortices

1B.5

Young C. Kwon* and William M. Frank
Pennsylvania State University, University Park, Pennsylvania

1. Introduction

Internally generated hurricane asymmetries have been known as the one of factors determining the structure and intensity of tropical storms. In the stable structure of a hurricane, outward propagating vortex Rossby waves in a hurricane core could produce inner rainbands and irregular-shaped eyewalls (Montgomery and Kallenbach, 1997). If the structure of a hurricane satisfies the necessary conditions of dynamic instabilities, barotropic and baroclinic instabilities might occur and they change the structure and intensity of a tropical storm via the interactions of a mean vortex and eddies (Schubert et al, 1999; Kwon and Frank, 2005).

Dynamic instability, however, is one special case of energy conversion processes, which is the exponential growth of eddy energy at the expense of the energy of a steady mean flow. A real hurricane case rarely stays in a steady state, and often does not satisfy the necessary condition of dynamic instabilities. Therefore, most of hurricanes rather experience non-exponential energy conversion than dynamic instabilities. In this study, the energy conversion processes are calculated using the energy equations* derived in this study and the effects of energy flows on a tropical cyclone will be discussed.

* Corresponding author address: Young C. Kwon, Dept. of Meteorology, 503 Walker, University Park, PA 16801, E-mail: yck108@psu.edu

2. Methodology

2.1 Model

An idealized hurricane-like vortex is simulated using Pennsylvania State University/National Center for Atmospheric Research (PSU/NCAR) Mesoscale Model (MM5). The grid resolution of the model is 6km, and the model domain is 1800km in both the north-south and east-west directions. The planetary boundary layer process is parameterized by Blackadar (1979) scheme, and the convections are explicitly described by a simple ice scheme which treats cloud water (or cloud ice, when temperature goes below freezing), rain water (or snow), and water vapor as explicit variables. The surface of whole model domain is an ocean with a constant sea surface temperature of 29°C. The simulation is performed on an f-plane valid on 17°N.

2.2 Experimental Design

An axisymmetric moist vortex in this study is designed using the same method of building the dry control vortex of Kwon and Frank (2005) except using the full-physics MM5. Hurricane Floyd (1999) is simulated with four nested domain, and the azimuthal averaging of model output is used to obtain an axisymmetric vortex.

The idealized moist vortex is simulated in the two different environments: One is in a clam environment, and the other is with weak vertical shear. For a simulation with shear, 5m/sec of the westerly vertical wind shear

from the bottom to top of the model is imposed over the whole model domain. The maximum vertical wind shear is located around $h=5\text{km}$ with surface $u=0$ and $u=5\text{m/sec}$ at the top of the model. The 48hour simulations of the moist vortex without shear (non-sheared vortex, hereafter) and with shear (sheared vortex, hereafter) are performed.

2.3 Energy Equations

To examine the energy flows of the sheared and non-sheared vortex, four energy equations on cylindrical coordinates are derived, an azimuthal mean kinetic energy (MKE) equation (Eq. 1), an eddy kinetic energy (EKE) equation (Eq. 2), an azimuthal mean available potential energy (MPE) equation (Eq. 3), and an eddy available potential energy (EPE) equation (Eq. 4).

$$\begin{aligned} \frac{\partial \bar{K}}{\partial t} = & -\frac{1}{r} \frac{\partial}{\partial r} [r(\overline{uK} + \overline{uu'u} + \overline{vv'v})] - \frac{\partial}{\partial p} (\overline{\omega K} + \overline{uu'\omega} + \overline{vv'\omega}) \\ & + (\overline{u'u'} \frac{\partial \bar{u}}{\partial r} + r\overline{u'v'} \frac{\partial}{\partial r} (\frac{\bar{v}}{r}) + \overline{u'\omega'} \frac{\partial \bar{u}}{\partial p} + \overline{v'\omega'} \frac{\partial \bar{v}}{\partial p} + \frac{\bar{u}}{r} \overline{v'v'}) - h\overline{\theta'_A \omega} + F_{\bar{K}} \end{aligned} \quad (1)$$

$$\begin{aligned} \frac{\partial \bar{K}'}{\partial t} = & -\frac{\partial}{\partial r} (\overline{uK'} + \overline{u'K'}) - \frac{\partial}{\partial p} (\overline{\omega K'} + \overline{\omega'K'}) - (\overline{u'u'} \frac{\partial \bar{u}}{\partial r} + r\overline{u'v'} \frac{\partial}{\partial r} (\frac{\bar{v}}{r}) \\ & + \overline{u'\omega'} \frac{\partial \bar{u}}{\partial p} + \overline{v'\omega'} \frac{\partial \bar{v}}{\partial p} + \frac{\bar{u}}{r} \overline{v'v'}) - h\overline{\theta'_A \omega'} + F_{\bar{K}'} \end{aligned} \quad (2)$$

$$\begin{aligned} \frac{\partial \bar{A}}{\partial t} = & -\frac{1}{r} \frac{\partial}{\partial r} \{r[A\bar{u} + (\frac{h}{s})^2 \overline{\theta'_A u' \theta'_A}]\} - \frac{\partial}{\partial p} [A\bar{\omega} + (\frac{h}{s})^2 \overline{\theta'_A \omega' \theta'_A}] + [(\frac{h}{s})^2 \overline{u' \theta'_A} \frac{\partial \bar{\theta}_A}{\partial r} \\ & + (\frac{h}{s})^2 \overline{\omega' \theta'_A} \frac{\partial \bar{\theta}_A}{\partial p}] + h\overline{\theta'_A \omega} + (\frac{h}{s})^2 \overline{\theta'_A Q} + F_{\bar{A}} \end{aligned} \quad (3)$$

$$\begin{aligned} \frac{\partial \bar{A}'}{\partial t} = & -\frac{1}{r} \frac{\partial}{\partial r} (rA'u) - \frac{\partial}{\partial p} (A'\bar{\omega}) - [(\frac{h}{s})^2 \overline{u' \theta'_A} \frac{\partial \bar{\theta}_A}{\partial r} + (\frac{h}{s})^2 \overline{\omega' \theta'_A} \frac{\partial \bar{\theta}_A}{\partial p}] \\ & + h\overline{\theta'_A \omega'} + (\frac{h}{s})^2 \overline{\theta'_A Q'} + F_{\bar{A}'} \end{aligned} \quad (4)$$

where u , v , and ω represent radial, tangential, and vertical velocity at pressure coordinates, respectively. Other notations are the same as a conventional use.

The energy conversion processes are represented by terms whose signs are opposite but have the same form in two different energy equations. For example, the third term of Eq. (1) and Eq. (2) represents barotropic process, energy conversion between MKE and EKE, while the third term of Eq. (3) and Eq. (4) represents baroclinic process, energy conversion between MPE and EPE.

3. Results

3.1 Evolution of Vortices

The central pressure of the non-sheared vortex is relatively steady in the range of 905mb to 925mb with a slight increase trend with time, while the intensity of the sheared vortex decreases rapidly with time (Fig. 1). The both vortices have similar intensity before $t=7.5\text{h}$, although vertical shear is imposed at the initial time. This delayed weakening of a sheared vortex well agrees with the previous studies (e.g., Frank and Ritchie, 2001). The vertical velocity and rain water in the sheared vortex have a distinct wavenumber-one structure (not shown). The area of the strongest upward motion and rain water is located at the northern side of the sheared vortex, downshear left, which well agrees with the previous studies.

3.2 Energy Flows

In the simulated moist vortices of this study, both barotropic and baroclinic processes are positive, which means the energy of a mean vortex transfers to the energy of eddies. In the non-shear case, the magnitude of the barotropic term is about one-order bigger than that of the baroclinic process. After imposing the environmental shear, both barotropic and barotropic terms

increase, which is consistent with the stronger eddy activity in the sheared vortex. In addition, the effect of vertical wind shear intensifies the baroclinic process proportionally more than the barotropic process.

The energy flows calculations in the early time period (averaged from $t=0\text{h}$ to $t=24\text{h}$) at the upper levels (integrated from $p=400\text{mb}$ to $p=100\text{mb}$) indicate the existence of baroclinic eddy life cycles in the sheared vortex. To show the baroclinic eddy life cycles, the time-height cross-section of the positive baroclinic and negative barotropic terms of the sheared vortex are provided in Fig. 2. The multiple baroclinic eddy life cycles are clearly seen in this picture mostly at the upper-level and before $t=24\text{hr}$. The four positive baroclinic processes are immediately followed by the four negative barotropic processes. The time interval between the maximum baroclinic and the minimum barotropic terms are about 2-3h.

4. Summary

The energy flows of an idealized axisymmetric moist vortex are analyzed using the energy equations derived in this study. Numerical simulations are performed using a stable, axisymmetric moist vortex with and without an environmental vertical shear. While the structure and intensity of the non-sheared vortex are relatively steady, those of the sheared vortex significantly change with time. The evolutions of the intensity and structure of the sheared vortex agree well with the previous studies, such as delayed weakening and wavenumber-one structure.

The temporal evolutions of the structures of thermal eddy and the mechanical eddy of the sheared vortex indicate the existence of baroclinic eddy life cycles similar to the baroclinically unstable dry vortex. The positive

baroclinic process intensifies eddies by decreasing the available potential energy of a mean vortex, which is proportional to the strength of the warm-core of tropical cyclones. After the available potential energy of the sheared vortex is sufficiently decreased by the positive baroclinic processes, the eddies at the upper levels begin to weaken because of the decline of energy source. The ventilation of the upper-level warm-core by this process results in weakening of the sheared vortex.

5. Reference

- Frank, W. M., and E. A. Ritchie, 2001: Effects of vertical wind shear on the intensity and structure of numerically simulated hurricanes. *Mon. Wea. Rev.*, **129**, 2249-2269.
- Kwon, Y. C. and W. M. Frank, 2005: Dynamic instabilities of simulated hurricane-like vortices and their impacts on the core structure of hurricanes. Part I: Dry Experiments. *J. Atmos. Sci.*, **62**, 3955-3973.
- Montgomery, M. T., and R. J. Kallenbach, 1997: A theory for vortex Rossby waves and its application to spiral bands and intensity changes in hurricanes. *Quart. J. Roy. Meteor. Soc.*, **123**, 435-465.
- Schubert, W. H., M. T. Montgomery, R. K. Shaft, T. A. Guinn, S. R. Fulton, J. P. Kossin, and J. P. Edwards, 1999: Polygonal eyewalls, asymmetric eye contraction, and potential vorticity mixing in hurricanes. *J. Atmos. Sci.*, **56**, 1197-1223.

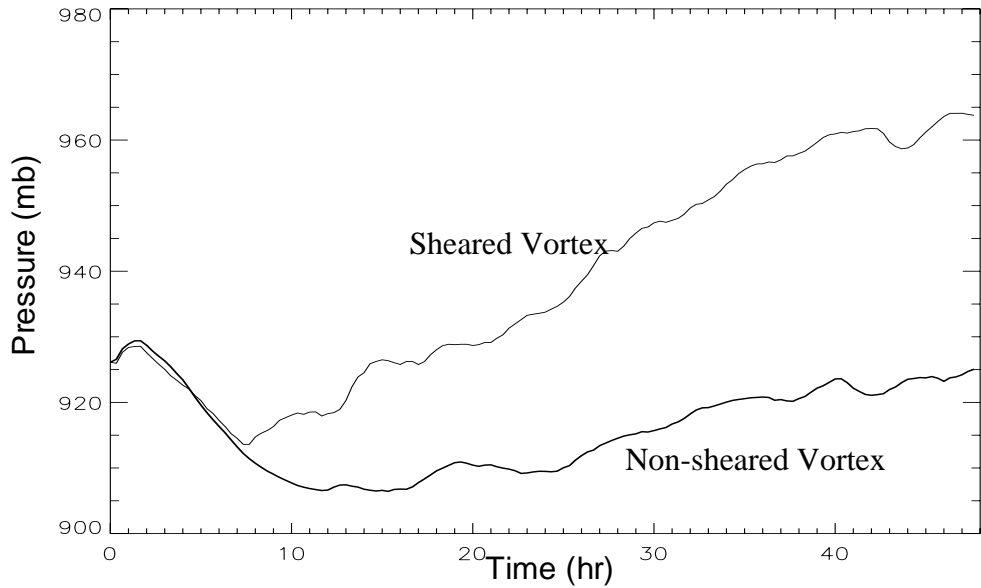


Fig. 1 Time series of the central pressure of the sheared (thin solid lines) and non-sheared vortices (thick solid lines).

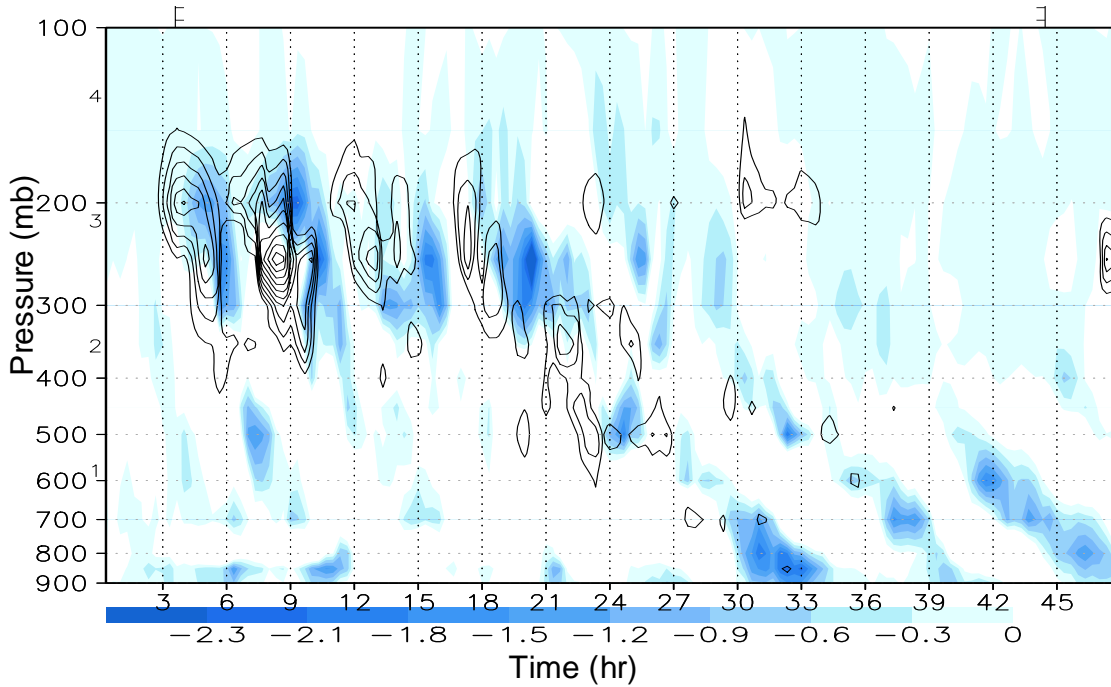


Fig. 2 Time-height cross-sections of the barotropic, baroclinic energy conversion terms for the sheared vortex. The values are radially averaged from $r=60\text{km}$ to 120km . The negative barotropic term (shaded) and positive baroclinic term (contour) are shown in this picture. The contour interval of the positive baroclinic term is $2 \times 10^{-3} \text{ J/sec}$.